Coupling Desorption Electrospray Ionization with Ion Mobility/Mass Spectrometry for Analysis of Protein Structure: Evidence for Desorption of Folded and Denatured States

Sunnie Myung,[†] Justin M. Wiseman,[‡] Stephen J. Valentine,[†] Zoltán Takáts,[‡] R. Graham Cooks,*[,‡] and David E. Clemmer*[,†]

Department of Chemistry, Indiana University, Bloomington, Indiana 47405, and Department of Chemistry, Purdue University, West Lafayette, Indiana 47907

Received: May 20, 2005; In Final Form: December 13, 2005

A desorption electrospray ionization (DESI) source has been coupled to an ion mobility time-of-flight mass spectrometer for the analysis of proteins. Analysis of solid-phase horse heart cytochrome *c* and chicken egg white lysozyme proteins with different DESI solvents and conditions shows similar mass spectra and charge state distributions to those formed when using electrospray to analyze these proteins in solution. The ion mobility data show evidence for compact ion structures [when the surface is exposed to a spray that favors retention of "*nativelike*" structures (50:50 water:methanol)] or elongated structures [when the surface is exposed to a spray that favors "*denatured*" structures (49:49:2 water:methanol:acetic acid)]. The results suggest that the DESI experiment is somewhat gentler than ESI and under appropriate conditions, it is possible to preserve structural information throughout the DESI process. Mechanisms that are consistent with these results are discussed.

Introduction

Ionization methods such as electrospray ionization (ESI),[1] matrix-assisted laser desorption ionization,[2] cold spray ionization,[3] and sonic spray ionization[4,5] make it possible to produce large intact biological ions in the gas phase. Recently, Takáts et al. developed desorption electrospray ionization (DESI),[6] a method for analysis of solids and condensed phase analytes that shares features of both desorption and spray ionization techniques. In one implementation of this method, macromolecules, typically on a nonconducting surface, are exposed to charged droplets and/or molecular cluster ions generated by ESI; this produces ions from the surface that can be transmitted through air into the mass spectrometer for analysis. An issue that arises for large ions is the extent to which structural elements of the macromolecule can be preserved throughout the ionization process. The ability to retain and characterize biologically relevant structures by mass spectrometry (MS) techniques is of fundamental interest to the field of protein (and macromolecular) folding[7−11] and has become topically important in the emerging area of biological arrays.[12]

There is now substantial evidence that suggests that under some conditions noncovalent structures, including a range of protein−protein, substrate−ligand, and fold types, can be preserved during the ESI process.[13−16] The charge state distributions that are produced by ESI appear to vary, depending upon the extent to which the protein is denatured in solution and on the mildness of the ionization technique. Intrinsic factors together with such experimental variables as solution pH,[15,16] solvent composition,[17] and temperature[18] have been related to the observed charge state distribution produced by ESI. It is generally assumed that denatured forms (having open structures with many exposed side chains that can be protonated or deprotonated) will exhibit higher charge states than more compact folded states.[9−11,15,16,19] For example, Chowdhury et al. observed a direct correlation of the observed charge state distribution with changes in the solution conformation of cytochrome *c* under different pH solvent conditions.[15]

A more direct approach to understanding the structures of proteins as they emerge from the ESI droplet into the gas phase is to characterize ion shapes and reactivities after ionization. The conformations of several model proteins (including the cytochrome *c* and lysozyme proteins chosen for study here) have been examined in detail by ion mobility and molecular modeling studies of cross section, as well as by isotopic exchange reactivity and other probes of stability and structure.[8−11,19−22] Overall, mobility studies of cytochrome *c* show that higher charge state ions exhibit elongated structures (primarily because these geometries reduce Coulombic repulsion and lower the energy of the system) whereas lower charge states exhibit more compact structures, which in some cases appear to have cross sections that are similar to those that would be expected if the ions retained much of their solution structure.[11,19,22] The native form of lysozyme contains four disulfide bonds that aid in stabilizing the folded state. When disulfide-intact ions are introduced into the gas phase with different solution and temperature conditions some evidence for denaturation can be found;[10] however, cross sections for compact and unfolded geometries are more similar than in the case of cytochrome *c*.[11,19]

In this paper we report the coupling of DESI to an instrument that combines ion mobility spectrometry (IMS) with MS. With this instrumental configuration it is possible to examine the charge state distributions and cross sections for protein ions in a single experiment. The combination of DESI with IMS allows us to address the interesting issue of how deposition onto a surface as a solid may influence structure. If proteins are highly denatured, compared to the ESI process, we would expect to see differences in the charge state distributions and cross

* To whom correspondence should be addressed. E-mail: clemmer@indiana.edu and cooks@purdue.edu.
[†] Indiana University.
[‡] Purdue University.

10.1021/jp052663e CCC: $33.50
Published on Web 02/14/2006

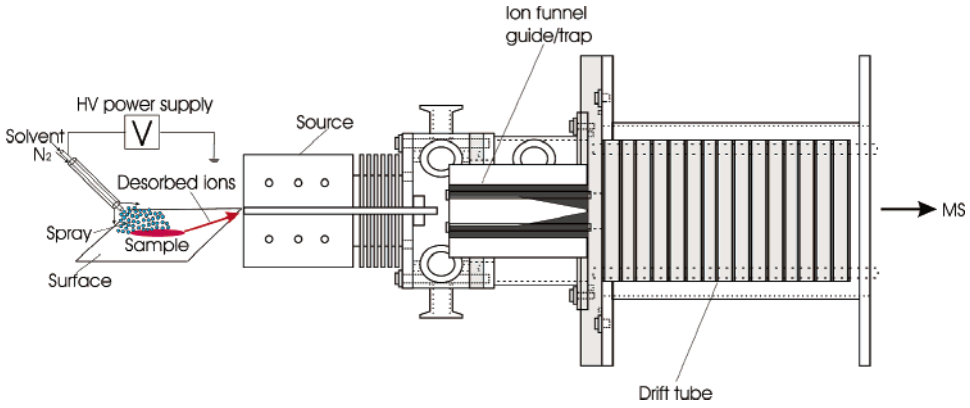

Figure 1. Schematic of a typical DESI-IMS-TOF experiment.

sections. The charge state distribution for lysozyme produced by DESI has been mentioned in the supplementary material for the original report of DESI.[6] The original study showed that when the protein surface is sprayed with a water:methanol:acetic acid solution that the distribution of charge states is similar to those found by ESI. Here, we follow up this study by comparing the ion mobility and charge state distributions of DESI generated ions with those recorded previously for ESI.[9−11,15,16,19] We study this system using two different spray conditions, both previously used for ESI studies: a solvent system favoring "*nativelike*" structures (i.e., no acid is added to the solution) and one that is denaturing. To test the role of DESI solvent composition on gas-phase ion structure in some detail we examine both cytochrome *c* and lysozyme. The primary finding of these studies is that both the charge state and ion mobility distributions for DESI-generated protein ions appear similar to distributions produced by ESI. This initial report about the nature of distribution of ions within a charge state is consistent with the notion that many elements of noncovalent structure that are accessible with ESI may be present with the DESI approach, making this an interesting new source for noncovalent ions. A simple mechanism (proposed for large biomolecules in the supplementary material associated with the original report)[6] consistent with these results is proposed.

Experimental Section

General. Detailed reviews of ion mobility techniques can be found elsewhere.[23] The experiment is outlined briefly here. Figure 1 shows a schematic of the DESI IMS-TOF configuration. Ions formed by DESI are extracted into a midpressure region (∼3 Torr) and focused into an ion funnel.[24] The rf potentials applied to the lenses combined with the dc potential at the end cap of the ion funnel allow ions from the continuous source to be accumulated (for ∼11−17 ms in this study) into a packet and then injected into the drift tube. The drift tube is 60 cm long and is operated with a 300 K He buffer gas pressure of 2.7 Torr. Inside the drift tube the ions drift under the influence of a weak field (∼13 $V \cdot cm^{-1}$) and are separated based on differences in their low-field mobilities through the buffer gas. Ions exit the drift tube through a differentially pumped orifice-skimmer cone region that is also designed to improve ion transmission (described previously)[25] and are transferred into the source region of a reflectron geometry time-of-flight (TOF) mass spectrometer. Flight times in the evacuated flight tube are much shorter (10 to 70 μs) than the drift times (1 to 20 ms) associated with the ion mobility separation. Thus, it is possible to record drift and flight times by using a nested approach.[26] The mass-to-charge (*m*/*z*) ratios of ions are determined from a standard multipoint calibration.

Sample Preparation and DESI Source. The DESI source is analogous in design to the one described previously.[6] Solutions of horse heart cytochrome *c* (97% purity, from Sigma) and chicken egg white lysozyme (90% purity, from Sigma) were prepared in water at a total concentration of $\sim 1.8 \times 10^{-5}$ to 2.1×10^{-5} M. All samples were deposited onto a polymethamethacrylate (PMMA) surface with a micropipet and were air-dried before analysis. Solvents consisting of either 50:50 water:methanol or 49:49:2 water:methanol:acetic acid (%volume) were sprayed at the sample plate at a volumetric flow rate of 3.5 μL/min. A high-pressure nebulizer was used to produce fine droplets (300 K, N_2 at a pressure of $\sim 6.9 \times 10^5$ Pa) sprayed at the surface. We note that in the present study the total ion intensity produced by DESI is about an order of magnitude lower than the intensity produced from an identical protein solution with ESI. This is mainly because the DESI setup is not optimal for the current IMS-MS configuration. Other DESI sources have been optimized such that intensities are comparable to signals produced by ESI.[6]

Effect of the Ion Funnel on IMS-MS Distributions. It is well-known that the rf voltages that are used for ion focusing in the ion funnel can lead to heating of ions. If such a condition were to exist in the present experiment then we would not be able to resolve differences in conformations that emerge during the DESI and ESI processes. We have carried out a series of experiments that ensure that rf heating is minimized. Under the conditions employed it is possible to observe differences in conformation that emerge from different solvent systems. These conditions appear to be very similar to our most gentle conditions that are found in our high-pressure ion mobility instrument. Overall, once the instrument has been optimized under minimal heating conditions the distributions for the well-studied cytochrome *c* and lysozyme systems make it possible to compare datasets. Unless otherwise noted, ion mobility distributions obtained here for ESI experiments are indistinguishable from the most gentle conditions found in high-pressure studies.

Results and Discussion

IMS-MS Distributions for Cytochrome *c* and Lysozyme Ions Formed by DESI. Figures 2 and 3 show typical two-dimensional nested ion mobility mass spectra obtained from DESI generated ions upon spraying surfaces deposited with cytochrome *c* and lysozyme, respectively. Here, we show data for conditions that utilize two solvent sprays: a 50:50 water:methanol solution (referred to as *nativelike since it favors retention of native protein structures*) and a 49:49:2 water:methanol:acetic acid solution (referred to as *denaturing*). We start by considering the cytochrome *c* data (Figure 2). These

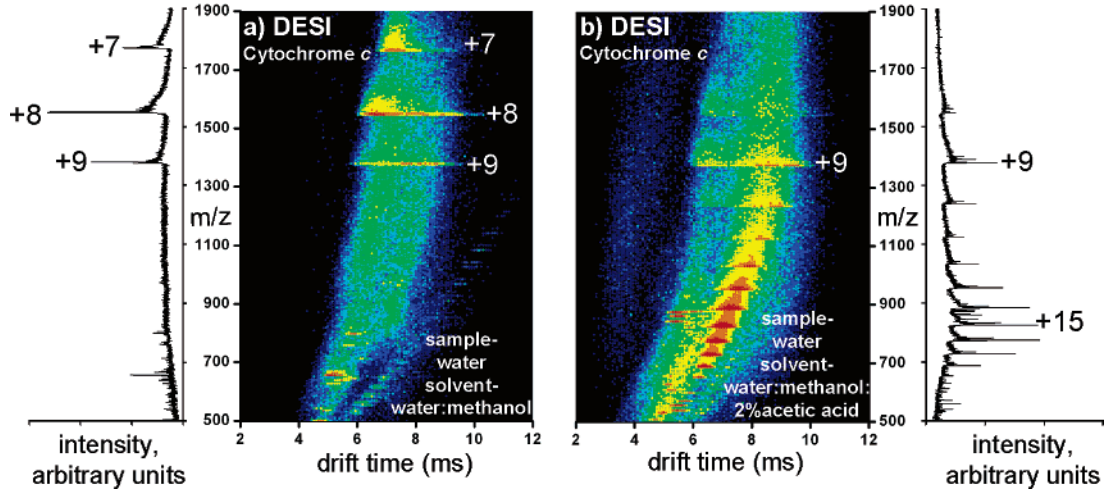

Figure 2. Two-dimensional plot of drift times (ms) versus *m*/*z* ratios obtained from a DESI-IMS-TOF experiment: (a) cytochrome *c* in water [solvent spray 50:50 water:methanol (% volume)] and (b) cytochrome *c* in water [solvent spray 49:49:2 water:methanol:acetic acid (% volume)]. The intensity of different features is shown by using a false color scheme in which the least intense features are represented in blue and the most intense features are represented in red. Different charge states are indicated within the 2D plot. The mass spectra were obtained by integrating the total two-dimensional data and normalizing them to the total ion intensity. See text for more detail.

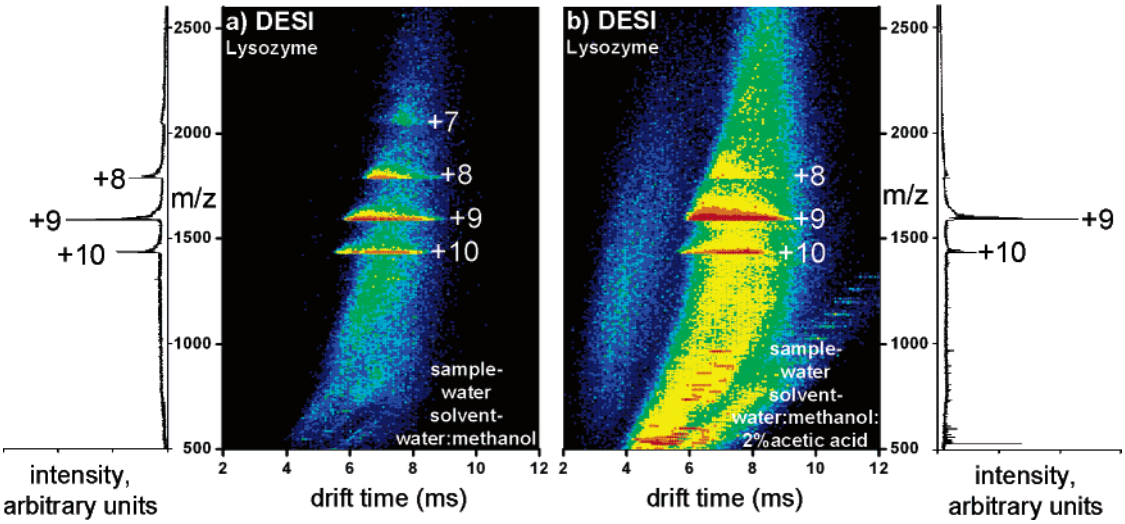

Figure 3. Two-dimensional plot of drift times (ms) versus *m*/*z* ratios obtained from a DESI-IMS-TOF experiment: (a) lysozyme in water [solvent spray 50:50 water:methanol (% volume)] and (b) lysozyme in water [solvent spray 49:49:2 water:methanol:acetic acid (% volume)]. All of the intensities and mass spectra are depicted the same way as in Figure 2. See text for detail.

data show a strong dependence upon the solvent used for the DESI process. Upon exposure to the *nativelike* condition we observe a charge state distribution dominated by the +7 to +9 charge states. From drift time distributions of each charge state (examined in more detail below), it is apparent that a significant fraction of these ions exist as relatively compact conformations. Both of these results are similar to results obtained by electrospraying cytochrome *c* from other nativelike solutions.[11,15,16,19]

In contrast, when a DESI solution containing 2% acetic acid is used we observe a bimodal charge state distribution, with maxima at the +9 and +15 charge states. Inspection of the drift time distributions for these charge states shows that the +9 charge state exists over a range of cross sections varying from those corresponding to compact to elongated structures. As discussed in more detail below, the higher charge states of +10 to +19 favor elongated geometries. These data are also similar to those obtained by electrospraying the protein directly from a water:methanol:acetic acid solution.[11,15,16,19]

Several other aspects of these plots are noteworthy. For example, we often observe relatively large backgrounds in these systems. Although the origin of the background ions is not entirely clear, the background ion signals appear to be somewhat larger in the present IMS-TOF instrument compared with data recorded in other DESI-MS instruments.[6] It is possible that some surface contamination is present in this system. The small features that are observed (and not attributed to protein ion charge states) are more apparent in data obtained operating DESI with denaturing solutions. Another interesting observation is that the ESI spectra recorded under the same conditions appear to show relatively more abundant low mass signals (more fragmentation) than the DESI spectra. This suggests that DESI may be a somewhat softer ionization method. Additional evidence for this is found in the fact that the major +8 charge state of cytochrome c shows more opened conformations under ESI conditions than in the DESI data (see below).

The results for lysozyme (Figure 3) show a somewhat different behavior. In this case, a narrow charge state distribution is produced, and this distribution changes only slightly for different DESI solutions. Although this result differs from the cytochrome *c* data as shown in Figure 2, the mass spectra are similar to those that we have measured before using ESI.[10] In the case of lysozyme, the changes in charge state distribution

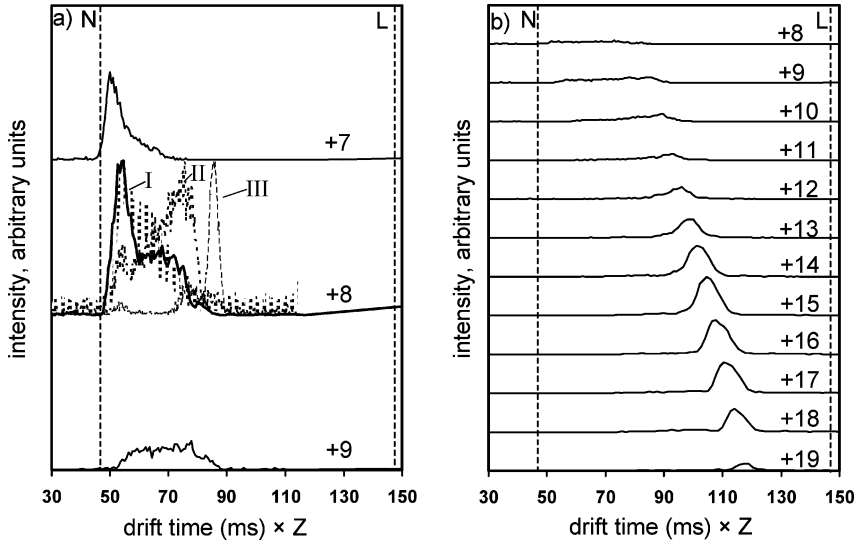

Figure 4. Drift time distributions (plotted on a scale where the drift time is multiplied by the charge state) obtained by integrating narrow regions of the IMS-TOF dataset over the region corresponding to various charge state ions for (a) cytochrome *c* in water [solvent spray 50:50 water: methanol (% volume)] and (b) cytochrome *c* in water [solvent spray 49:49:2 water:methanol:acetic acid (% volume)]. In part a, previously reported ESI ion mobility distributions (ref 19a) with different injection voltages for the +8 charge state are incorporated into parta (middle) as dashed lines. These data have been normalized to the present data by a calibration to other known systems. The various injection voltages are indicated as I−III representing 60, 80, and 120 V, respectively. As shown in both parts a and b, the two dashed lines labeled N and L near 46.7 and 57.9 ms are the drift times that are calculated for the native conformation found in solution and linear geometry, respectively. Both values were calculated by using the projection approximation (ref 29). The intensities are normalized to the total count followed by normalization to the maximum intensity from each dataset. See text for more details.

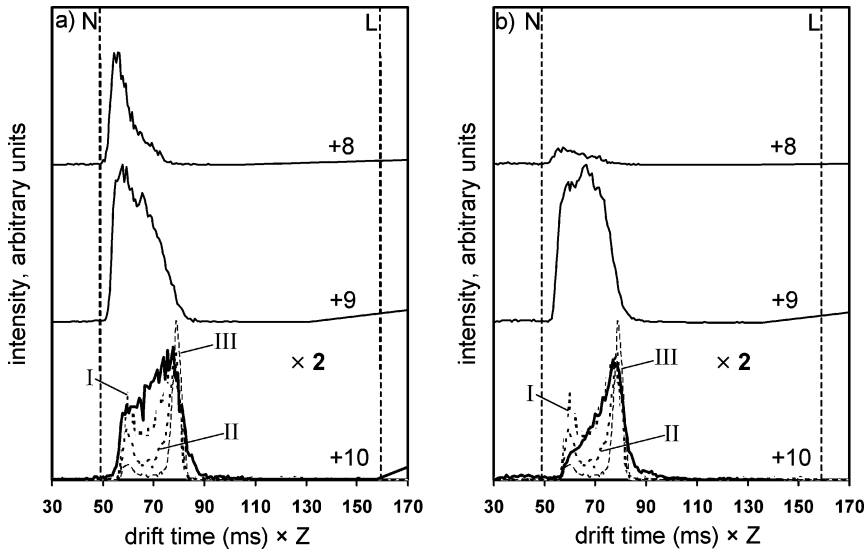

Figure 5. The drift mobility distribution (plotted on a scale where the drift time is multiplied by the charge state) obtained by integrating the narrow regions of the IMS-TOF dataset over the region corresponding to various charge state ions for (a) lysozyme in water [solvent spray 50:50 water:methanol (% volume)] and (b) lysozyme in water [solvent spray 49:49:2 water:methanol:acetic acid (% volume)]. Previously reported ESI ion mobility distributions (ref 10) with different injection voltages for the +10 charge state are incorporated into the figure as dashed lines. The various injection voltages are indicated as I−III representing 60, 70, and 90 V, respectively. The two dashed lines labeled N and L near 48.7 and 158.4 ms are the drift times that is calculated for the crystal structure in solution and a near-linear conformer, respectively. The values and the intensities of peaks are depicted the same way as in Figure 4. See text for details.

in this system are mediated by the four covalent disulfide linkages between the 6−127, 30−115, 64−80, and 76−94 cystine residues[27]—therefore, the available protonation sites and conformations are restricted for disulfide-intact lysozyme.

Overall, the most remarkable features of Figures 2 and 3 are that the DESI ionization process appears to produce mass spectra that are qualitatively similar to those produced by ESI. That is, the changes in charge state distributions that are observed upon varying the solution conditions (i.e., adding acid) are comparable for ESI and DESI. However, there are also differences between the data for the two techniques as discussed below.

Comparison of DESI and ESI Ion Mobility Distributions for Specific Charge States. A more detailed understanding of this system can be obtained by examining the ion mobility distributions for individual charge states. Figures 4 and 5 compare ion mobility distributions for specific charge states when ions are produced by DESI and ESI. It is important to begin this discussion by mentioning that it is possible to influence the gas-phase structures of protein ions by varying a number of experimental parameters. Most important to the present study is what happens during the injection process. Several groups have shown that as ions are injected from a low-

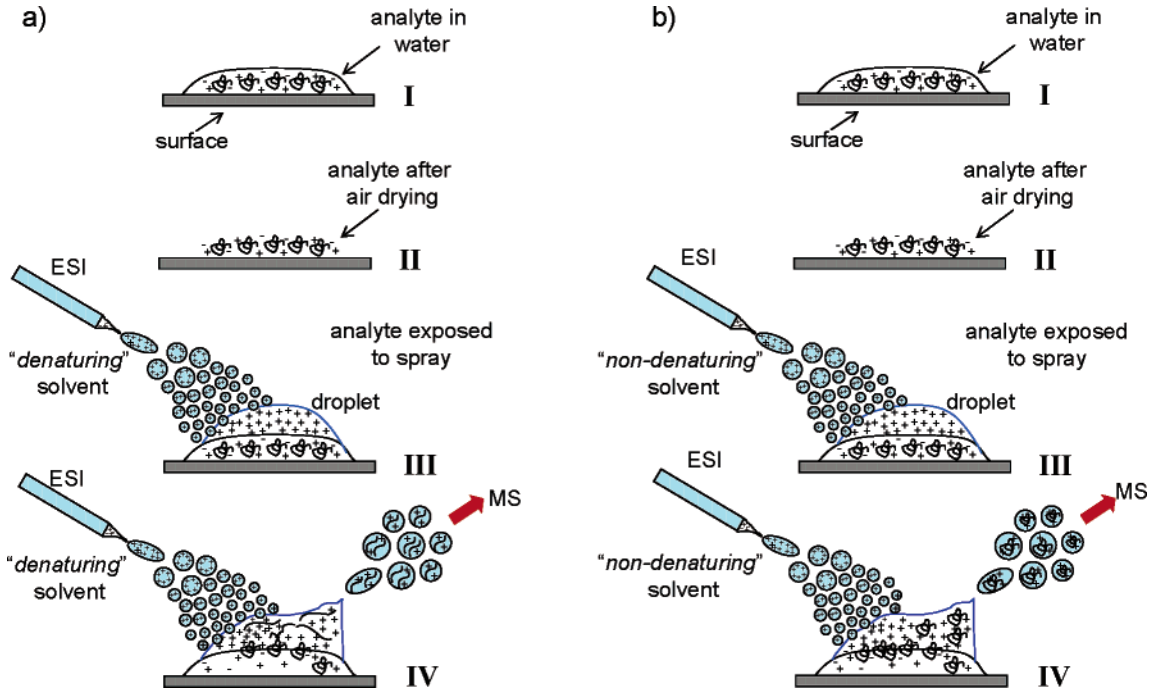

Figure 6. Schematic representation of the proposed "*droplet pick-up*" mechanism for the desorption electrospray ionization process with two different solvent spray conditions described as (a) "*denaturing*" [49:49:2 water:methanol:acetic acid (% volume)] and (b) "*nativelike*" [50:50 water:methanol (% volume)] . The ionization process is illustrated as follows: (I) the analyte is deposited onto a surface, (II) it is air-dried before analysis, (III) this is followed by exposure to the solvent spray, and (IV) finally the analyte is picked up by the droplet before being electrostatically removed from the surface into the source of the instrument. It is in steps III and IV that the protein ions undergo structural changes because of the spray conditions. See text for more details.

pressure ion source into the drift tube they are rapidly heated as their kinetic energy is thermalized by collisions with the buffer gas.[10,11,19,28] Further collisions cool the ions to the buffer gas temperature. Figure 4 shows typical ion-mobility distributions as a function of charge state for cytochrome *c* with different DESI spray solvents. For comparison, these results are shown in a modified drift time (the drift time multiplied by the charge state), which normalizes for differences in the effective drift field (*zE*) for different charge states. Intensity distributions for each of the drift slices in Figures 4 and 5 is shown on an arbitrary intensity scale.

In cytochrome *c*, the lowest observed charge state is the +7 arriving at ~50.2 ms, a value that is close to the drift time calculated from a projection approximation[29] estimate for the coordinates of the crystal structure[30] (note than an exact hard sphere scattering[31] estimate would yield slightly longer drift times). The peak shape is relatively narrow and similar to peak shapes observed for $[M + 7H]^{7+}$ produced by ESI. For the +8 charge state there is evidence for multiple conformations: a narrow peak at ~55 ms and a shoulder at longer times associated with more diffuse structures, although to less of an extent than is the case with ESI. The distribution for the +9 charge state is broad, extending from ~50 to 90 ms. This indicates the presence of ions containing a range of different geometries.

Also shown in Figure 4a are several ESI distributions for the $[M + 8H]^{8+}$ ion formed under different injection energy conditions.[19a] At high injection energies (III) this ion favors elongated geometries (at ~83 ms); although these ions are significantly more compact than the drift time estimated for an extreme linear geometry (L, having no secondary or tertiary structure), the ions must have relatively little remaining tertiary structure. By contrast, highly folded states (I) of the $[M + 8H]^{8+}$ ions dominate under gentle injection conditions. It appears that ions formed by DESI most resemble low-energy injection conditions. That is DESI ions appear to exist as relatively compact ions that have not been exposed to energizing collisions.

In other recent work, we have examined ESI generated ions in an ion trap and monitored conformations as a function of trapping times.[32] Under these conditions the $[M + 8H]^{8+}$ ions favor compact geometries at short trapping times; however, after delay times of ~30 to 40 ms they open up to favor more extended structures. Thus, it would appear that the distribution of ions that is produced by DESI for $[M + 8H]^{8+}$ ions most closely resembles an array of ions that are preserved under gentle injection conditions and exist for short times after they are formed by ESI.

Upon adding 2% acetic acid to the DESI solvent the signal for the lower charge state ions decreases significantly. Under these conditions the distribution around the +12 charge state arriving at ~95.4 ms starts to appear. As the number of attached protons increases the peak shifts to larger times. This shift is consistent with the increase in cross section that has been reported previously for the charge state increase from +10 to +19.[11,19]

Ion mobility distributions for the +8 through +10 charge states of lysozyme are shown in Figure 5. Under conditions that favor *nativelike* conformations the +8 charge state exhibits a narrow distribution arriving at ~55.1 ms, while only a small and broad peak is observed for the *denaturing* conditions. The effects of solvent spray conditions are not as dramatic as shown for cytochrome *c*. However, there are slight differences in the mobility distribution of the +9 charge state. As shown in Figure 5, the +9 peak is most intense at ~57.9 ms when the *nativelike* condition is used whereas the maximum for the +9 charge state is centered at ~65.8 ms when acid is involved. Although the distribution is broad for both cases, the dominance of shorter initial arrival time suggests that a more compact structure is

favored for the +9 charge state ion when *nativelike* conditions are employed. Even with the presence of four disulfide bonds, the acid in the microdroplet has enough interactions with the +9 charge state ion to produce a slight shift in the drift time distribution. For comparison, previously reported ESI results for the +10 charge state with different injection energies are shown in Figure 5.[10] Under the *nativelike* conditions the +10 charge state is dominated by a peak at ~78 ms. The position of these peaks as well as the proportion of the shoulder to the most intense peak indicates that the best agreement of the *nativelike* peak is with the ESI generated peak using low injection energy of 60 V into the drift tube. The *denaturing* conditions produce a slight variation in the proportion of the peak intensities for the higher mobility peak to the most intense peak arriving at ~78 ms suggesting a closer resemblance to the mobility distribution obtained by using higher injection energies. These results suggest that disulfide-intact lysozyme distribution produced by DESI agrees well with ESI mobility distribution when similar conditions are employed.

Implications Regarding the DESI Mechanism of Proteins. The results presented above for DESI and ESI analysis of cytochrome *c* and lysozyme can be used to provide some insight into protein ion formation by DESI. Three mechanisms that are associated with formation of different types of ions were proposed in the initial DESI report: (1) a *droplet pick-up* mechanism; (2) chemical sputtering involving charge transfer between the droplets and the surface; and (3) a mechanism where volatile molecules are first desorbed from the surface and subsequently ionized by gas-phase charge transfer (or other ion−molecule reactions). The process that was suggested to apply to proteins and is most consistent with the results presented here is the *droplet pick-up* mechanism. We have illustrated a hypothetical process by which protein ions would be formed in Figure 6. In this case the dried sample surface is electrosprayed with a specific solution. As charged microdroplets impact the surface, protein molecules become dissolved in the solution or simply adhere to the droplet surface and are carried away from the surface by the nebulizing gas jet. In this way, gas phase protein ions are formed by mechanisms proposed for electrospray ionization of large molecules. The subsequent desolvation of the protein-bearing microdroplet leaving the surface parallels processes that occur when electrospraying protein-containing microdroplets from solution. This accounts for a remarkable feature of our results in that both the charge state and ion mobility distributions are similar to those produced by ESI. In summary, when the surface proteins are exposed to a water:methanol solution they desorb out of the microdroplet as relatively low charge state ions with compact conformations, whereas when the proteins are exposed to a solution containing 2% acetic acid, a distribution of high-charge state ions with elongated structures is favored. This is apparent for the lysozyme system (which is conformationally restricted by the disulfide bridges) and is relatively dramatic for the cytochrome *c* system. It appears, however, that DESI produces gas-phase protein ions that can be relatively less sensitive to the solvent as indicated by retaining some native conformations under acidic conditions. This may be partially due to the heterogeneous nature of the spray impacting the surface.

A question that emerges in this mechanism is in regard to when the protein ions are emitted from the surface. A significant feature of traditional ESI is that small droplets are emitted from a very sharp needle, where the local fields are significant enough to create the characteristic ESI Taylor cone. Recent work from Grimm and Beauchamp shows that when neutral droplets (containing proteins) are exposed to strong transient fields it is possible to extract distributions of charge states from the neutral droplet.[33] Other studies[34] show that as a charged droplet dries it may spontaneously deform and charge is emitted in bursts of much smaller droplets from the ends of deformed droplets with ellipsoid structures. We note that a deformation of the surface could be induced by the charged particles that are impacting upon the surface, consistent with the initial splashing mechanism that was proposed. In any case, a key feature of the ions that are produced is that they take on the characteristics of the solvent from which they were emitted. For a folded structure, such as a protein, this requires that the protein was at some point dissolved into the solvent system that leads to gas-phase ion formation similar to ESI processes.

Conclusions

We have presented the first experiments in which a DESI source has been coupled to an IMS-TOF instrument. This is a very straightforward coupling that essentially was functional the first time it was attempted. An important advantage of this combination is the ability to separate the distribution of DESI ions prior to MS analysis. The first example focused on the analysis of two well-characterized proteins: cytochrome *c* and lysozyme. The analysis shows that the charge state distributions and ion mobility distributions are highly dependent upon the solvents that are used to spray the surface. When a 50:50 water: methanol solution is used to spray the surface, the ion distribution is dominated by low-charge state ions having relatively compact gas-phase conformations; when 2% acetic acid is added to the spray solution higher charge states, having more open conformations, are favored. The variation in the gas-phase conformations is most dramatic for cytochrome *c*. Smaller variations are observed for lysozyme, presumably because this protein is conformationally restricted by four disulfide bonds. Overall, the charge state and ion mobility distributions appear to be very similar to those formed by ESI, and the dependence upon solution conditions is similar. Therefore, a mechanism in which proteins are emitted from charged droplets on the surface appears to be consistent with these data.

While the present work has focused on proteins, the approach can also be relevant for a range of other types of species, including tryptic peptides as well as other small analytes. We are currently examining the utility of the combined DESI-IMS-TOF approach for these types of systems.

Acknowledgment. Financial support for this work was provided by the National Science Foundation (Grant Nos. CHE-0078737 and CHE 97-32670).

References and Notes

(1) Fenn, J. B.; Mann, M.; Meng, C. K.; Wong, S. F.; Whitehouse, C. M. *Science* **1989**, *246*, 64.

(2) Karas, M.; Hillenkamp, F. *Anal. Chem.* **1988**, *60*, 2299.

(3) Yamaguchi, K. *J. Mass. Spectrom.* **2003**, *38*, 473.

(4) Hirabayashi, A.; Sakairi, M.; Koizumi, H. *Anal. Chem.* **1995**, *67*, 2878. Hirabayashi, A.; Hirabayashi, Y.; Sakairi, M.; Koizumi, H. *Rapid Commun. Mass Spectrom.* **1996**, *10*, 1703. Björkman, H. T.; Edlund, P.; Jacobsson, S. P. *Anal. Chim. Acta* **2002**, *468*, 263.

(5) Takáts, Z.; Nanita, S. C.; Cooks, R. G.; Schlosser, G.; Vekey, K. *Anal. Chem.* **2003**, *75*, 1514.

(6) Takáts, Z.; Wiseman, J. M.; Gologan, B.; Cooks, R. G. *Science* **2004**, *306*, 471. Details of the methods and additional experimental results are available as supporting online material at *http://www.sciencemag.org*.

(7) van Duijin, E.; Bakkes, P. J.; Heeren, R. M. A.; van den Heuvel, R. H. H.; van Heerikhuizen, H.; van der Vies, S. M.; Heck, A. J. R. *Nature*

Methods **2005**, *2*, 371. Benesch, J. L. P.; Sobott, F.; Robinson, C. V. *Anal. Chem.* **2003**, *75*, 2208. Hernandez, H.; Robinson, C. V. *J. Biol. Chem.* **2001**, *276*, 46685.

(8) Breuker, K.; Oh, H. B.; Horn, D. M.; Cerda, B. A.; McLafferty, F. W. *J. Am. Chem. Soc.* **2002**, *124*, 6407. Suckau, D. S.; Shi, Y.; Beu, S. C.; Senko, M. W.; Quinn, J. P.; Wampler, F. M., III; McLafferty, F. W. *Proc. Natl. Acad. Sci. U.S.A.* **1993**, *90*, 790.

(9) Gross, D. S.; Schnier, P. D.; Rodriguez-Cruz, S. E.; Fagerquist, C. K.; Williams, E. R. *Proc. Natl. Acad. Sci. U.S.A.* **1996**, *93*, 3143.

(10) Valentine, S. J.; Anderson, J. G.; Ellington, A. D.; Clemmer, D. E. *J. Phys. Chem. B* **1997**, *101*, 3891.

(11) Jarrold, M. F. *Acc. Chem. Res.* **1999**, *32*, 360. Shelimov, K. B.; Clemmer, D. E.; Hudgins, R. R.; Jarrold, M. F. *J. Am. Chem. Soc.* **1997**, *119*, 2240.

(12) Gembitsky, D. S.; Lawlor, K.; Jacovina, A.; Yaneva, M.; Tempst, P. *Mol. Cell. Proteomics* **2004**, *3*, 1102. Blake, T. A.; Zheng, O.; Wiseman, J. M.; Zoltan, T.; Guymon, A. J.; Kothari, S.; Cooks, R. G. *Anal. Chem.* **2004**, *76*, 6293. Mitchell, P. *Nat. Biotechnol.* **2002**, 20, 225. Washburn, M. P. *Nat. Biotechnol.* **2003**, *21*, 1156.

(13) Rostom, A. A.; Robinson, C. V. *J. Am. Chem. Soc.* **1999**, *121*, 4718. Loo, J. A. *Mass Spectrom. Rev.* **1997**, *16*, 1. Ganem, B.; Li, Y.-T.; Henion, J. D. *J. Am. Chem. Soc.* **1991**, *113*, 6294. Ganem, B.; Li, Y.-T.; Henion, J. D. *J. Am. Chem. Soc.* **1991**, *113*, 7818. Katta, V.; Chait, B. T. *J. Am. Chem. Soc.* **1993**, *115*, 6317. Smith, D. L.; Zhang, Z. *Mass Spectrom. Rev.* **1994**, *13*, 411. Eckart, K.; Spiess, J. *J. Am. Soc. Mass Spectrom.* **1995**, *6*, 912.

(14) Takáts, Z.; Wiseman, J. M.; Gologan, B.; Cooks, R. G. *Anal. Chem.* **2004**, *76*, 4050. Takáts, Z.; Nanita, S. C.; Cooks, R. G. *Angew. Chem., Int. Ed.* **2003**, *42*, 3521.

(15) Chowdhury, S. K.; Katta, V.; Chait, B. T. *J. Am. Chem. Soc.* **1990**, *112*, 9012.

(16) Wagner, D. S.; Anderegg, R. J. *Anal. Chem.* **1994**, *66*, 706. Konermann, L.; Silva, E. A.; Sogbein, O. F. *Anal. Chem.* **2001**, *73*, 4836. Babu, K. R.; Moradian, A.; Douglas, D. J. *J. Am. Soc. Mass Spectrom.* **2001**, *12*, 317. Konermann, L.; Douglas, D. J. *J. Am. Soc. Mass Spectrom.* **1998**, *9*, 1248. Konermann, L.; Douglas, D. J. *Rapid Commun. Mass Spectrom.* **1998**, *12*, 435.

(17) Loo, J. A.; Loo, R. R. O.; Udseth, H. R.; Edmonds, C. G.; Smith, R. D. *Rapid Commun. Mass Spectrom.* **1991**, *5*, 101. Iavarone, A. T.; Jurchen, J. C.; Williams, E. R. *J. Am. Soc. Mass Spectrom.* **2000**, *11*, 976.

(18) Miraz, U. A.; Cohen, S. L.; Chait, B. T. J. *Anal. Chem.* **1993**, *65*, 1. LeBlanc, J. C. Y.; Beuchemin, D.; Siu, K. W. M.; Guevremont, R.; Berman, S. S. *Org. Mass Spectrom.* **1991**, *5*, 582. Rockwood, A. S.; Busman, M.; Udseth, H. R.; Smith, R. D. *Rapid Commun. Mass Spectrom.* **1991**, *5*, 582.

(19) (a) Valentine, S. J.; Clemmer, D. E. *J. Am. Chem. Soc.* **1997**, *119*, 3558. (b) Clemmer, D. E.; Hudgins, R. R.; Jarrold, M. F. *J. Am. Chem. Soc.* **1995**, *117*, 10141.

(20) Wood, T. D.; Chorush, R. A.; Wampler, F. M., III; Little, D. P.; O'Connor, P. B.; McLafferty, F. W. *Proc. Natl. Acad. Sci. U.S.A.* **1995**, *92*, 2451. McLafferty, F. W.; Guan, Z.; Haupts, U.; Wood, T. D.; Kelleher, N. L. *J. Am. Chem. Soc.* **1998**, *120*, 4732.

(21) Winger, B. E.; Light-Wahl, J. J.; Rochwood, A. L.; Smith, R. D. *J. Am. Chem. Soc.* **1992**, *114*, 5897. Cassady, C. J.; Carr, S. R. *J. Mass Spectrom.* **1996**, *31*, 247. Ogorzalek Loo, R. R.; Smith, R. D. *J. Am. Soc. Mass Spectrom.* **1994**, *5*, 207. Sullivan, P. A.; Axelsson, J.; Altmann, S.; Quist, A. P.; Sunqvist, B. U. R.; Reimann, C. T. *J. Am. Chem. Soc. Mass Spectrom.* **1996**, *7*, 329.

(22) Covey, T. R.; Douglas, D. J. *J. Am. Soc. Mass Spectrom.* **1993**, *4*, 616.

(23) St. Louis, R. H.; Hill, H. H. *Crit. Rev. Anal. Chem.* **1990**, *21*, 321. Wyttenbach, T.; Bushnell, J. E.; Bowers, M. T. *J. Am. Chem. Soc.* **1998**, *120*, 5098. Clemmer, D. E.; Jarrold, M. F. *J. Mass. Spectrom.* **1997**, *32*, 577. Hoaglund Hyzer, C. S.; Counterman, A. E.; Clemmer, D. E. *Chem. Rev.* **1999**, *99*, 3037. Jarrold, M. F. *Annu. Rev. Phys. Chem.* **2000**, *51*, 179.

(24) Kim, T.; Tolmachev, A. V.; Harkewicz, R.; Prior, D. C.; Anderson, G. A.; Udseth, H. R.; Smith, R. D.; Bailey, T. H.; Rakov, S.; Futrell, J. H. *Anal. Chem.* **2000**, *72*, 2247.

(25) Lee, Y. J.; Hoaglund-Hyzer, C. S.; Taraszka, J. A.; Zientara, G. A.; Counterman, A. E.; Clemmer, D. E. *Anal. Chem.* **2001**, *73*, 3549.

(26) Hoaglund, C. S.; Valentine, S. J.; Sporleder, C. R.; Reilly, J. P.; Clemmer, D. E. *Anal. Chem.* **1998**, *70*, 2236.

(27) Jauregui-Adell, J.; Jollès, J.; Jollès, P. *Biochim. Biophys. Acta* **1965**, *107*, 97.

(28) Hunter, J. M.; Fye, J. L.; Jarrold, M. F.; Bower, J. E. *Phys. Rev. Lett.* **1994**, *73*, 2063.

(29) von Helden, G.; Hsu, M. T.; Gotts, N.; Bowers, M. T. *J. Phys. Chem.* **1993**, *97*, 8182. Wyttenbach, T.; von Helden, G.; Batka, J. J., Jr.; Carlat, D.; Bowers, M. T. *J. Am. Soc. Mass Spectrom.* **1997**, *8*, 275.

(30) Bushnell, G. W.; Louie, G. V.; Brayer, G. D. *J. Mol. Biol.* **1990**, *214*, 585.

(31) Shvartsburg, A. A.; Jarrold, M. F. *Chem. Phys. Lett.* **1996**, *261*, 86.

(32) Badman, E. R.; Hoaglund-Hyzer, C. S.; Clemmer, D. E. *Anal. Chem.* **2001**, *73*, 6000.

(33) Grimm, R. L.; Beauchamp, J. L. *J. Phys. Chem. B* **2003**, *107*, 14161.

(34) Duft, D.; Achtzehn, T.; Müller, R.; Huber, B. A.; Leisner, T. *Nature* **2003**, *421*, 128.